

KIF5B-ALK, a Novel Fusion Oncokinase Identified by an Immunohistochemistry-based Diagnostic System for ALK-positive Lung Cancer

Kengo Takeuchi,¹ Young Lim Choi,³ Yuki Togashi,¹ Manabu Soda,³ Satoko Hatano,¹ Kentaro Inamura,¹ Shuji Takada,³ Toshihide Ueno,³ Yoshihiro Yamashita,³ Yukitoshi Satoh,² Sakae Okumura,² Ken Nakagawa,² Yuichi Ishikawa,¹ and Hiroyuki Mano^{3,4}

Abstract Purpose: EML4-ALK is a transforming fusion tyrosine kinase, several isoforms of which have been identified in lung cancer. Immunohistochemical detection of EML4-ALK has proved difficult, however, likely as a result of low transcriptional activity conferred by the promoter-enhancer region of *EML4*. The sensitivity of EML4-ALK detection by immunohistochemistry should be increased adequately.

Experimental Design: We developed an intercalated antibody-enhanced polymer (iAEP) method that incorporates an intercalating antibody between the primary antibody to ALK and the dextran polymer-based detection reagents.

Results: Our iAEP method discriminated between tumors positive or negative for *EML4-ALK* in a test set of specimens. Four tumors were also found to be positive for ALK in an archive of lung adenocarcinoma ($n = 130$) and another 4 among fresh cases analyzed in a diagnostic laboratory. These 8 tumors were found to include 1 with *EML4-ALK* variant 1, 1 with variant 2, 3 with variant 3, and 2 with previously unidentified variants (designated variants 6 and 7). Inverse reverse transcription-PCR analysis revealed that the remaining tumor harbored a novel fusion in which intron 24 of *KIF5B* was ligated to intron 19 of *ALK*. Multiplex reverse transcription-PCR analysis of additional archival tumor specimens identified another case of lung adenocarcinoma positive for *KIF5B-ALK*.

Conclusions: The iAEP method should prove suitable for immunohistochemical screening of tumors positive for ALK or ALK fusion proteins among pathologic archives. Coupling of PCR-based detection to the iAEP method should further facilitate the rapid identification of novel ALK fusion genes such as *KIF5B-ALK*.

Gene fusion is a major mechanism of carcinogenesis in hematologic malignancies and sarcomas (1). Identification of the BCR-ABL fusion kinase, which is generated as a result of the balanced chromosome anomaly $t(9;22)(q34;q11)$ in chronic myelogenous leukemia (2), has thus been followed by the discovery of many fusion-type oncogenes (3). In contrast, it has remained unclear whether such translocation-dependent fusion-type oncogenes also play a major role in the pathogenesis of epithelial tumors. Recently, however, almost 50% of prostate cancer cases have been suggested to harbor gene fusions involving ETS transcription factor loci

(4), and we have discovered a recurrent chromosome translocation, $inv(2)(p21p23)$, in non-small cell lung cancer (NSCLC) that results in the production of an EML4-ALK fusion-type protein tyrosine kinase (PTK; refs. 5–8).

Forced expression of EML4-ALK in lung epithelial cells induced the rapid development of hundreds of lung cancer nodules in mice, and peroral administration of inhibitors of the PTK activity of EML4-ALK was shown to clear such tumors from the lungs, demonstrating the pivotal role of EML4-ALK in the pathogenesis of NSCLC positive for this fusion kinase (9). This latter observation also supports the clinical application of ALK

Authors' Affiliations: ¹Division of Pathology, The Cancer Institute, Japanese Foundation for Cancer Research and ²Department of Thoracic Surgical Oncology, Thoracic Center, Cancer Institute Hospital, Japanese Foundation for Cancer Research, Tokyo, Japan; ³Division of Functional Genomics, Jichi Medical University, Tochigi, Japan; and ⁴CREST, Japan Science and Technology Agency, Saitama, Japan

Received 12/15/08; revised 1/23/09; accepted 2/1/09; published OnlineFirst 4/21/09.

Grant support: Supported in part by Grants-in-Aid for Scientific Research from the Ministry of Education, Culture, Sports, Science, and Technology of Japan as well as by grants from the Japan Society for the Promotion of Science; the Ministry of Health, Labor, and Welfare of Japan; the National Institute of Biomedical Innovation of Japan; the Smoking Research Foundation of Japan; and the Vehicle Racing Commemorative Foundation of Japan.

The costs of publication of this article were defrayed in part by the payment of page charges. This article must therefore be hereby marked *advertisement* in accordance with 18 U.S.C. Section 1734 solely to indicate this fact.

Note: Supplementary data for this article are available at Clinical Cancer Research Online (<http://clincancerres.aacrjournals.org/>).

Current address of Y. Satoh: Department of Thoracic Surgery, Kitasato University School of Medicine, Kanagawa 228-8520, Japan.

Requests for reprints: Kengo Takeuchi, Division of Pathology, The Cancer Institute, Japanese Foundation for Cancer Research, Tokyo 135-8550, Japan. Phone: 81-3-3520-0111; Fax: 81-3-3570-0558; E-mail: kentakeuchi-tyk@umin.net.

© 2009 American Association for Cancer Research.

doi:10.1158/1078-0432.CCR-08-3248

Translational Relevance

Immunohistochemistry (IHC) is a reliable and relatively easy diagnostic tool to detect pathologic proteins in paraffin-embedded tissues. We have recently discovered an oncogenic fusion tyrosine kinase EML4-ALK in ~5% of non-small cell lung cancer cases. In contrast to the sensitive detection of other ALK fusions, such as NPM-ALK in anaplastic large cell lymphoma, however, IHC-mediated identification of EML4-ALK has been difficult, probably owing to the low expression level of the protein. To overcome such limitation, we here developed an intercalated antibody-enhanced polymer (iAEP) method, which is simple, yet provides high sensitivity in the IHC-mediated detection of EML4-ALK. With iAEP, in addition to the faithful detection of all non-small cell lung cancer specimens known to be positive for EML4-ALK, we have further identified specimens carrying novel variants of EML4-ALK or an unknown oncogenic fusion, KIF5B-ALK. Therefore, iAEP would provide a reliable and sensitive means to detect ALK fusions in human cancers.

inhibitors (6, 10) to treat EML4-ALK-positive lung cancer in humans. It should be noted, however, that multiple isoforms of EML4-ALK, generated mainly as a result of diversity in the breakpoint-fusion point within *EML4* (6, 8, 11, 12), have been identified in NSCLC specimens. The accurate diagnosis of EML4-ALK-positive tumors will therefore require detection of

all in-frame fusions between *EML4* and *ALK* cDNAs, as exemplified by our multiplex reverse transcription- and PCR-based detection system for *EML4-ALK* (8).

Given that, in many pathology laboratories, most specimens submitted for histopathologic diagnosis are stored as formalin-fixed, paraffin-embedded tissue, the DNA or RNA of which may be substantially degraded, it is desirable to develop a suitable and sensitive means to detect EML4-ALK in such samples. An immunohistochemistry-based diagnostic system is one potential approach to such screening. In contrast to the efficient detection of NPM-ALK fusion proteins in anaplastic large cell lymphoma specimens with such an approach (13), however, many researchers have encountered difficulty in detecting ALK fusion proteins in lung tissue by immunohistochemical analysis (14), possibly as a result of weak transcriptional activity of the promoter-enhancer region of *EML4* that drives the expression of *EML4-ALK* compared with that of the *NPM* promoter. We have now attempted to establish a sensitive screening system for ALK fusion protein-positive tumors with an immunohistochemical approach. Furthermore, with such an approach, we unexpectedly discovered a novel *ALK* fusion gene, *KIF5B-ALK*, in NSCLC.

Materials and Methods

Samples. As a test set of samples for the development of sensitive immunohistochemical detection of EML4-ALK, we examined specimens from 11 patients with NSCLC positive for *EML4-ALK* (previously analyzed in ref. 8) and 10 patients with NSCLC negative for the fusion

Table 1. Immunohistochemical staining of EML4-ALK-positive or EML4-ALK-negative NSCLC specimens and quantitation of *ALK* mRNA

Tumor ID	EML4-ALK variant	Staining intensity						ALK mRNA level	
		ALK1	ALK1 with iAEP	5A4	5A4 with iAEP	SP8	SP8 with iAEP	5' region	3' region
#4808	V1	-	+	-	+	-	+	1.3	57.3
#9034	V1	-	++	+	++	-/+	++	0	83.3
#9968	V1	-	+	-	+	-	+	15.9	150.1
#2374	V2	-	++	-/+	++	-/+	++	1	182.3
#3121	V2	-	++	-/+	++	-/+	++	0	118.6
#4180	V2	-	++	-/+	++	-/+	++	1.4	124.5
#2075	V3	-	++	-/+	++	-/+	++	7	72
#7969	V3	+	+++	++	+++	+	++	3.6	52.7
#9616	V3	-/+	++	+	++	+	++	5.7	33.8
#8398	V4	-	++	-/+	++	-/+	++	0	118.6
#8993	V5	-	++	-/+	++	-/+	++	1.1	61.4
NC #1	NA	-	-	-	-	-	-/+	1	1
NC #2	NA	-	-	-	-	-	-/+	1.2	5.5
NC #3	NA	-	-	-	-	-/+	+	0.9	8.8
NC #4	NA	-	-	-	-/+	-/+	++	4.1	1.4
NC #5	NA	-	-	-	-	-	+	0.6	2.2
NC #6	NA	-	-	-	-	-	+	0.3	1.1
NC #7	NA	-	-	-	-	-/+	+	4.8	2.7
NC #8	NA	-	-	-	-	-	+	1.7	3.8
NC #9	NA	-	-	-	-	-	+	1.5	3.3
NC #10	NA	-	-	-	-/+	-/+	++	2.5	3

NOTE: Tumor specimens of the test cohort were subjected to immunohistochemical staining with the antibody preparations ALK1, 5A4, or SP8 according to the standard protocol or by the iAEP method. Staining intensity is represented as follows: +++, strongly positive; ++, positive; +, weakly but definitely positive; -/+, indeterminate; -, negative. The abundance of ALK mRNA in the specimens was determined by real-time RT-PCR analysis with the primers targeted to the 5' or 3' regions, which correspond to the extracellular and intracellular portions, respectively, of ALK; data are normalized relative to the NC (negative control) #1 specimen. Abbreviation: NA, not applicable.

Downloaded from http://aacrjournals.org/clinccancerres/article-pdf/15/9/3143/1988621/3143.pdf by guest on 22 May 2022

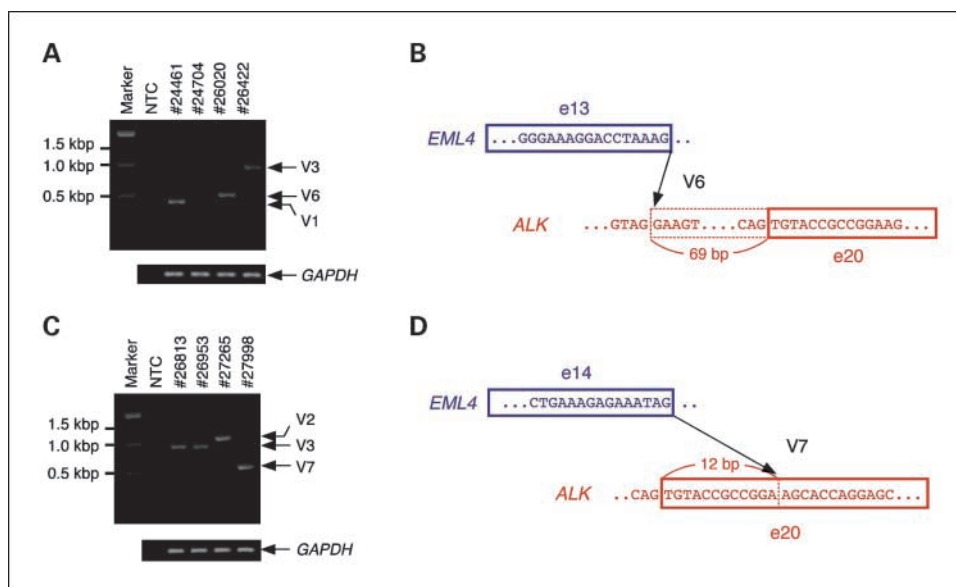


Fig. 1. Identification of novel variants of *EML4-ALK*. **A**, multiplex RT-PCR analysis of all possible in-frame fusions between *EML4* and *ALK* was done with the four specimens of lung adenocarcinoma in the validation cohort that were positive for immunostaining with 5A4 by the iAEP method (*top*). In addition to the detection of *EML4-ALK* variants (V)1 and 3 in tumor IDs #24461 and #26422, respectively, a novel PCR product (variant 6) was obtained with tumor ID #26020, whereas no product was obtained with tumor ID #24704. The *GAPDH* cDNA was also amplified as a control for each specimen (*bottom*). Tumor IDs (*top*) and the size of DNA markers (*bottom*; 100-bp ladder) are shown. *Right*, the positions of *EML4-ALK* variants and the PCR product for *GAPDH*. *NTC*, no-template control. **B**, fusion point for *EML4-ALK* variant 6 cDNA. Exon (e) 13 of *EML4* is fused to intron 19 of *ALK* at a position 69 bp upstream of exon 20. **C**, multiplex RT-PCR analysis as in **A** for the 4 specimens of lung adenocarcinoma that were identified as positive for immunostaining with 5A4 by the iAEP method in routine diagnostic screening. Tumor IDs #26813 and #26953 were shown to be positive for variant 3 of *EML4-ALK*, whereas #27265 was positive for variant 2. Tumor ID #27998 yielded a PCR product corresponding to a novel variant (variant 7) of *EML4-ALK*. **D**, fusion point of *EML4-ALK* variant 7 cDNA. Exon 14 of *EML4* is fused to nucleotide 13 of exon 20 of *ALK*.

gene. The former cohort comprised 3 cases each for *EML4-ALK* variants 1, 2, and 3 as well as one case each for variants 4 and 5. As a validation set of samples, we examined specimens from 130 consecutive patients with lung adenocarcinoma, from whom written informed consent was obtained. All specimens were collected with the approval of the ethics committee at the Cancer Institute Hospital (Tokyo, Japan), and the study was approved by the institutional review board of the Japanese Foundation for Cancer Research. Surgically removed cancer specimens were routinely fixed in 20% neutralized formalin and embedded in paraffin. Total RNA was extracted from the corresponding snap-frozen specimens and purified with the use of an RNeasy Mini kit (Qiagen).

Intercalated antibody-enhanced polymer method. Formalin-fixed, paraffin-embedded tissue was sliced at a thickness of 4 μ m, and the sections were placed on silane-coated slides. Five antibody preparations specific for the intracellular region of ALK (ALK1 from Dako, 5A4 and SP8 from Abcam, ZAL4 from Zymed, and p80 from Nichirei) were evaluated for immunohistochemical staining according to standard protocols with the use of a dextran polymer reagent (anti-rabbit or anti-mouse immunoglobulin EnVision+DAB system; Dako). On the basis of their reactivity in such experiments, three antibodies (ALK1, 5A4, and SP8) were selected for development of the intercalated antibody-enhanced polymer (iAEP) method as follows. For antigen retrieval, the slides were heated for 40 min at 97°C in Target Retrieval Solution (pH 9.0; Dako). They were then incubated at room temperature first with Protein Block Serum-free Ready-to-Use solution (Dako) for 10 min and then with antibodies to ALK for 30 min. To increase the sensitivity of detection, we included an incubation step of 15 min at room temperature with rabbit polyclonal antibodies to mouse immunoglobulin (Dako) or mouse antibodies to rabbit immunoglobulin (Dako), as appropriate. The immune complexes were then detected with the dextran polymer reagent and an AutoStainer instrument (Dako).

Detection of *EML4-ALK* and *KIF5B-ALK* cDNAs and characterization of their protein products is described in Supplementary Methods.

Results

Development of the iAEP method. A specimen of NPM-ALK-positive anaplastic large cell lymphoma was subjected to immunohistochemical staining with 5 different antibody preparations specific for ALK (ALK1 at a 1:20 dilution, 5A4 at 1:50, SP8 at 1:100, ZAL4 at 1:200, or p80 at 1:100) by the EnVision+DAB polymer method. All antibody preparations stained both the nucleus and cytoplasm of the lymphoma cells, whereas ZAL4 also reacted with normal mesenchymal cells (data not shown). In addition, the staining intensity with p80 was relatively low. We therefore selected ALK1, 5A4, and SP8 for initial development of a detection system for *EML4-ALK*.

Immunohistochemical analysis of a test set of samples (11 specimens of *EML4-ALK*-positive NSCLC and 10 specimens of *EML4-ALK*-negative NSCLC) with these 3 antibody preparations revealed negative to marginally positive reactivity with *EML4-ALK* by a conventional staining protocol based on the EnVision+DAB system (Supplementary Fig. S1; Table 1). We therefore incorporated an intercalating antibody before the EnVision+DAB system and applied this iAEP method to the same set of specimens. All three antibody preparations detected *EML4-ALK* in all *EML4-ALK*-positive cases in the test cohort (Supplementary Fig. S1; Table 1). However, SP8 also reacted with most of the *EML4-ALK*-negative specimens (Supplementary Fig. S2; Table 1), rendering it unsuitable for large-scale screening. Furthermore, a low level of nonspecific background staining of nontumor cells was apparent in all sections stained with ALK1.

We selected ALK1 and 5A4 for examination of a validation set of samples (a consecutive series of 130 lung adenocarcinoma

specimens). Four cases of this cohort were positive for staining with both antibodies by the iAEP method. Again, most of the other specimens also showed a low level of background staining with ALK1, whereas only a few did so with 5A4. We therefore selected 5A4 to detect EML4-ALK with the iAEP method and included this approach in our routine diagnostic service at the pathology division of The Cancer Institute during the study period, thereby identifying four additional cases of lung adenocarcinoma positive for staining with 5A4.

Identification of variants 6 and 7 of EML4-ALK. The four specimens recognized by 5A4 in the validation set (IDs #24461, #24704, #26020, and #26422) were examined for the presence of EML4-ALK transcripts with our multiplex reverse transcription-PCR (RT-PCR) screening system, which was designed to capture all possible in-frame fusions between EML4 and ALK at the cDNA level (8). Three cases (#24461, #26020, and #26422) were positive for EML4-ALK cDNAs (Fig. 1A), and nucleotide sequencing of the PCR products revealed that #24461 and #26422 tumors harbored variants 1 and 3 of EML4-ALK, respectively. The cDNA derived from tumor #26020, however, contained exon 13 of EML4 as well as a portion of intron 19 and exon 20 of ALK, corresponding to a previously unidentified fusion variant (designated variant 6) of EML4 and ALK

(Supplementary Fig. S3A; Fig. 1B). The fusion of exon 13 of EML4 to a position 69 bp upstream of exon 20 of ALK in this fusion cDNA would be expected to constitute an in-frame fusion between the two genes. Although there were no reported mRNAs or expressed sequence tags containing intron 19 of ALK in the sequence databases, the genomic sequence surrounding the fusion point in this intron is AG-GA (Fig. 1B), which conforms to the consensus sequence for a splicing acceptor site, suggesting that this position of intron 19 may act as a cryptic acceptor site for RNA splicing.

Similar analysis by multiplex RT-PCR and sequence determination revealed that the additional 4 ALK-positive cases identified by our routine pathologic diagnostic service comprised one case (tumor ID #27265) with variant 2 of EML4-ALK, 2 cases (#26813 and #26953) with variant 3, and 1 case (#27998) with another novel variant (designated variant 7), in which exon 14 of EML4 is fused to nucleotide 13 of exon 20 of ALK (Supplementary Fig. S3B; Fig. 1C and D). Genomic PCR analysis of the specimens positive for variants 6 and 7 of EML4-ALK cDNA confirmed the presence of genomic rearrangements responsible for the fusion events detected at the cDNA level (data not shown).

Identification of KIF5B-ALK as a novel ALK fusion gene. Whereas tumor #24704 of the validation cohort was strongly positive for ALK immunostaining by the iAEP method, multiplex RT-PCR analysis failed to amplify a specific product from this sample. We therefore examined the possibility that this tumor might harbor an ALK fusion gene other than EML4-ALK. We subjected the sample to an inverse RT-PCR analysis and obtained a PCR product containing both exon 24 of KIF5B and exon 20 of ALK. KIF5B is located on the short arm of human chromosome 10 and encodes member 5B of the kinesin family of proteins. To confirm the presence of a KIF5B-ALK fusion gene in this tumor, we directly amplified the fusion point of the KIF5B-ALK cDNA by RT-PCR with one primer targeted to exon 24 of KIF5B and the other to exon 22 of ALK. A single PCR product with the expected size of 546 bp was obtained (Fig. 2A). Nucleotide sequencing of the product further confirmed the fusion point of KIF5B-ALK at the cDNA level (data not shown).

KIF5B is a component of a motor protein complex that is associated with microtubules and mediates the transport of organelles within eukaryotic cells (15). It consists of an amino terminal motor domain followed by a neck region and a stalk region, the latter of which directly mediates homodimerization of KIF5B (Fig. 2B). Fusion of exons 1 to 24 of KIF5B to exon 20 of ALK would be expected to result in the production of a fusion protein consisting of almost the entire KIF5B sequence ligated to the intracellular region of ALK. It might therefore also be expected that KIF5B-ALK would undergo homodimerization mediated by the stalk region of KIF5B, with consequent activation of the kinase function of ALK, similar to the case of EML4-ALK, in which homo-oligomerization and activation are mediated by the amino terminal coiled-coil domain of EML4 (5, 8).

We next modified our multiplex RT-PCR method so that it could detect both EML4-ALK and KIF5B-ALK fusion mRNAs. In addition to a forward primer targeted to the boundary of exons 23 and 24 of KIF5B (to amplify the identified KIF5B-ALK fusion point), we included another forward primer targeted to exon 10 of KIF5B to detect potential novel fusion cDNAs for

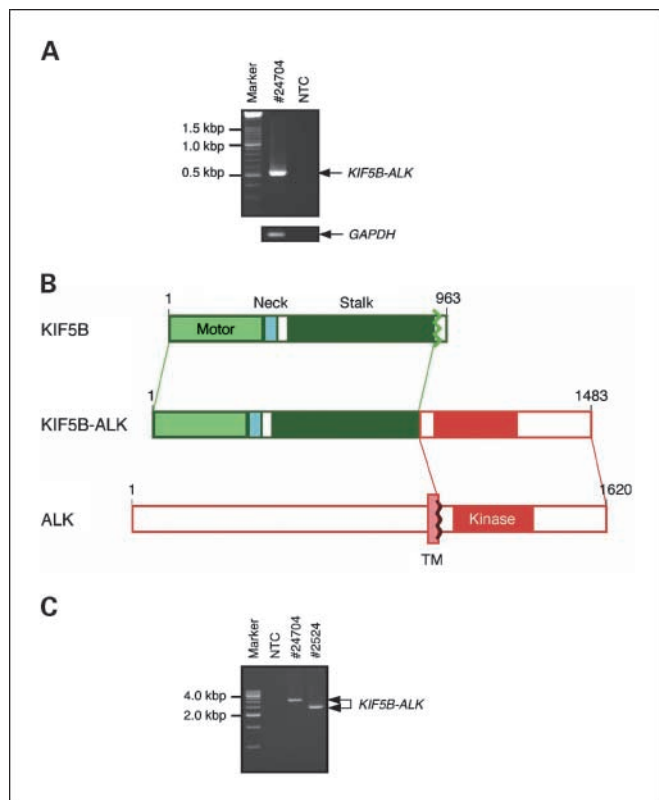
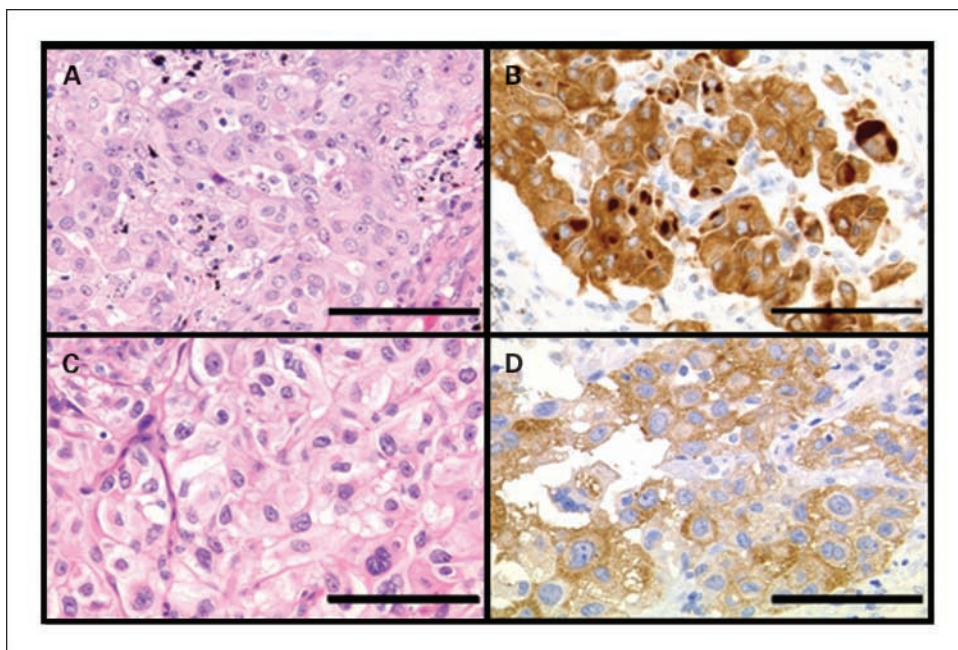


Fig. 2. Discovery of a KIF5B-ALK fusion gene associated with lung cancer. **A**, RT-PCR analysis of tumor ID #24704 with a forward primer targeted to exon 24 of KIF5B and a reverse primer targeted to exon 20 of ALK. Marker, 100-bp ladder. **B**, structure of KIF5B-ALK. KIF5B consists of an amino terminal ATP-dependent motor domain followed by a neck region and a stalk region containing seven coiled-coil domains. A chromosome translocation, t(2;10)(p23;p11), generates a fusion protein in which the entire motor domain and neck and stalk regions of KIF5B are joined to the intracellular region of ALK (containing the tyrosine kinase domain). Numbers indicate amino acid positions of each protein. *TM*, transmembrane domain. **C**, PCR analysis of genomic DNA from tumors #24704 and #2524 with primers flanking the putative fusion point of KIF5B-ALK. Marker, 500-bp ladder.

Fig. 3. Histopathology of KIF5B-ALK–positive lung adenocarcinoma. Sections of tumors #24704 (A and B) and #2524 (C and D) were stained with H&E (A and C) or subjected to immunohistochemical analysis with 5A4 by the iAEP method (B and D). Some cancer cells of tumor #24704 contained intracytoplasmic macroglobular spots strongly positive for KIF5B-ALK (B). Some tumor cells showed a perinuclear halo positive for KIF5B-ALK (D). Scale bars, 100 μ m.



KIF5B-ALK proteins containing a partial stalk region of KIF5B (given that the stalk region contains seven coiled-coil domains, a partial stalk region may still allow homodimerization of KIF5B-ALK). This newly designed multiplex RT-PCR assay was then applied both to the eight specimens found in this study to harbor *EML4-ALK* (7 cases) or *KIF5B-ALK* (#24704) and to the panel of cancer specimens including 253 samples of lung adenocarcinoma, 111 samples of other types of lung cancer, and 292 samples of tumors from 10 other organs, which was studied previously (8). Our modified multiplex RT-PCR method detected all 8 cases shown to be positive for *EML4-ALK* or *KIF5B-ALK* in the present study as well as 11 cases known to harbor various *EML4-ALK* fusion genes in the previous cohort (data not shown). The modified multiplex RT-PCR assay also identified one case (#2524) of lung adenocarcinoma harboring *KIF5B-ALK* among the previous cohort. We thus identified two cases positive for *KIF5B-ALK* among a total of 383 cases of lung adenocarcinoma (2 of 383 = 0.52%). Genomic rearrangement responsible for the identified *KIF5B-ALK* cDNAs was also confirmed in these two cases by genomic PCR analysis. The PCR products differed between the 2 cases, indicative of distinct breakpoints and fusion points within intron 24 of *KIF5B* and intron 19 of *ALK* (Fig. 2C).

Histopathology of KIF5B-ALK–positive lung adenocarcinoma. Histopathologic analysis of the two cases of *KIF5B-ALK*–positive lung adenocarcinoma revealed papillary structures, whereas the acinar pattern with prominent mucin production typically apparent in *EML4-ALK*–positive cases (7) was rarely observed. The individual cancer cells contained abundant eosinophilic cytoplasm and a large vesicular nucleus with one or two prominent nucleoli, and they were generally larger than those observed in *EML4-ALK*–positive cases (Supplementary Fig. S4A; Fig. 3A and C). Lymphatic invasion was prominent in tumor #24704, and the tumor cells in the lymphatic vessels contained an eccentric nucleus and a perinuclear eosinophilic globule (Supplementary Fig. S4A). Immunohistochemical detection of KIF5B-ALK with 5A4 by the iAEP method revealed

a diffuse cytoplasmic staining in all of the cancer cells. Some cells manifested an uneven staining profile, with a perinuclear halo (Supplementary Fig. S4B; Fig. 3D) or macroglobular spots (Fig. 3B), neither of which was observed in tumors positive for *EML4-ALK* (8).

Fluorescence in situ hybridization analysis of KIF5B-ALK–positive tumors. To confirm further the genomic rearrangement in the two tumors positive for *KIF5B-ALK*, we did three fluorescence *in situ* hybridization assays: an *ALK* split assay, a *KIF5B* split assay, and a *KIF5B-ALK* fusion assay. The results for all three assays were consistent with the presence of a t(2;10)(p23;p11) responsible for the generation of *KIF5B-ALK* (Fig. 4). Cancer cells of tumor #24704 thus exhibited one isolated 3′-*ALK* signal and one isolated 5′-*KIF5B* signal in the *ALK* split assay and the *KIF5B* split assay, respectively, whereas they manifested one merged signal in the *KIF5B-ALK* fusion assay. Cancer cells of tumor #2524 exhibited at least two merged signals, indicative of possible amplification of the fusion gene. Neither an isolated 3′-*KIF5B* signal nor an isolated 5′-*ALK* signal was detected in the split assays for either case, suggesting that the derivative chromosome 2 harboring the *ALK-KIF5B* fusion gene may have been deleted after the balanced translocation between chromosomes 2 and 10.

Transforming activities of EML4-ALK variants 6 and 7 and of KIF5B-ALK. To isolate full-length cDNAs for the new variants of *EML4-ALK*, we did RT-PCR analysis with a forward primer targeted to the 5′ untranslated region of *EML4* cDNA and a reverse primer targeted to the 3′ untranslated region of *ALK* cDNA as described previously (6, 8). From oligo(dT)-primed cDNA preparations of tumor IDs #26020 or #27998, we isolated cDNAs of 3365 and 3435 bp, corresponding to variants 6 and 7 of *EML4-ALK*, respectively (data not shown). Similarly, a full-length cDNA of 4479 bp for *KIF5B-ALK* was obtained by RT-PCR analysis from tumor ID #2524. Nucleotide sequencing of these cDNAs confirmed that each of them would be expected to produce a functional PTK, with a predicted molecular size of 119,380 Da for *EML4-ALK* variant 6 (Supplementary Fig. S3A),

122,220 Da for EML4-ALK variant 7 (Supplementary Fig. S3B), and 167,903 Da for KIF5B-ALK (Supplementary Fig. S5).

Recombinant retroviruses encoding each of these fusion PTKs were generated and used to infect cultured 3T3 fibroblasts. Infection with the viruses encoding EML-ALK variant 6, EML4-ALK variant 7, or KIF5B-ALK, but not that with the empty virus, resulted in the formation of dozens of transformed foci *in vitro* (Fig. 5). As positive controls for focus formation, EML4-ALK variant 1 and NPM-ALK each yielded a similar number of transformed foci.

The same set of 3T3 cells was injected into nude mice for an *in vivo* tumorigenicity assay. All fusion PTKs induced s.c. tumors at all injection sites within an observation period of 20 days (Fig. 5), confirming the transforming potential of the novel variants of EML4-ALK as well as that of KIF5B-ALK.

Discussion

Immunohistochemical detection of ALK fusion proteins has been applied successfully to analysis of anaplastic large cell lymphoma and inflammatory myofibroblastic tumors, with the mouse monoclonal antibody ALK1 being most widely used for this purpose. However, many researchers were not able to reliably detect EML4-ALK in NSCLC specimens with this same immunohistochemical technique (14). Even if NSCLC specimens were positive for such staining, its intensity was usually

low and varied substantially among sections of the same tumor, rendering the current standard technique unsuitable for screening of NSCLC specimens. This low sensitivity for the detection of EML4-ALK may be attributable to the low level of *EML4* transcriptional activity (see, for example, a public database for serial analysis of gene expression)⁵ or to instability of EML4-ALK in cells.

However, given that immunohistochemical analysis is a convenient means to detect a protein of interest in pathology laboratories, it is desirable to establish a sensitive and accurate screening system for ALK fusion proteins based on this approach. Several candidate techniques with improved sensitivity, such as tyramide signal amplification (16), have been recently proposed. These techniques generally require multiple steps, however, which can compromise reproducibility and render them unsuitable for screening in routine pathologic diagnosis.

We have now achieved a moderate increase in the sensitivity of immunohistochemical detection of ALK fusion proteins by including antibodies to mouse or rabbit immunoglobulin as an intercalating reagent between the primary antibody and the EnVision+DAB polymer detection system. This iAEP method allowed the detection of EML4-ALK fusion proteins in all 11 specimens positive for *EML4-ALK* in our test cohort. This simple method can be readily done in ordinary diagnostic pathology laboratories. Although we selected the mouse monoclonal antibody 5A4 for immunohistochemistry by the iAEP method, other antibodies may be more suitable for routine diagnostic analysis with a modified version of this approach.

All antibodies used in the present study are specific for the intracellular region of ALK and so would be expected to detect both EML4-ALK and wild-type ALK. It is therefore possible that positive staining with 5A4 by the iAEP method does not reflect only the presence of ALK fusion proteins. To address this issue, we determined the amount of *ALK* mRNA with primers targeted to the 5' or 3' regions of *ALK* cDNA separately (whereas the latter would be expected to amplify cDNAs for both wild-type *ALK* and *ALK* fusion genes, the former would be expected to amplify only that of wild-type *ALK*). None of the *EML4-ALK*-positive specimens in the test set of samples yielded a substantial amount of wild-type *ALK* cDNA (although tumor #9968 may express the wild-type gene at a low level), suggesting that our iAEP method with 5A4 detected EML4-ALK proteins rather than wild-type ALK in the positive specimens. For ALK-rich tissues such as the brain or spinal cord (17), however, it would be important to determine which proteins are recognized by 5A4 in iAEP analysis.

We identified 8 tumors positive for staining with 5A4 by the iAEP method among the validation set of samples ($n = 130$) and the fresh cases subjected to routine diagnostic testing. Although 5 of these specimens harbored known EML4-ALK variants, the remaining three were found to express novel ALK fusion proteins, including EML4-ALK variants 6 (#26020) and 7 (#27998) and KIF5B-ALK (#24704). These results thus showed that sensitive immunohistochemical analysis was superior to PCR-based methods for detecting novel ALK fusion constructs among tumor specimens. This conclusion was further supported by the fact that neither *EML4-ALK* nor *KIF5B-ALK* was identified in the iAEP-negative cases by our modified multiplex RT-PCR assay (data not shown).

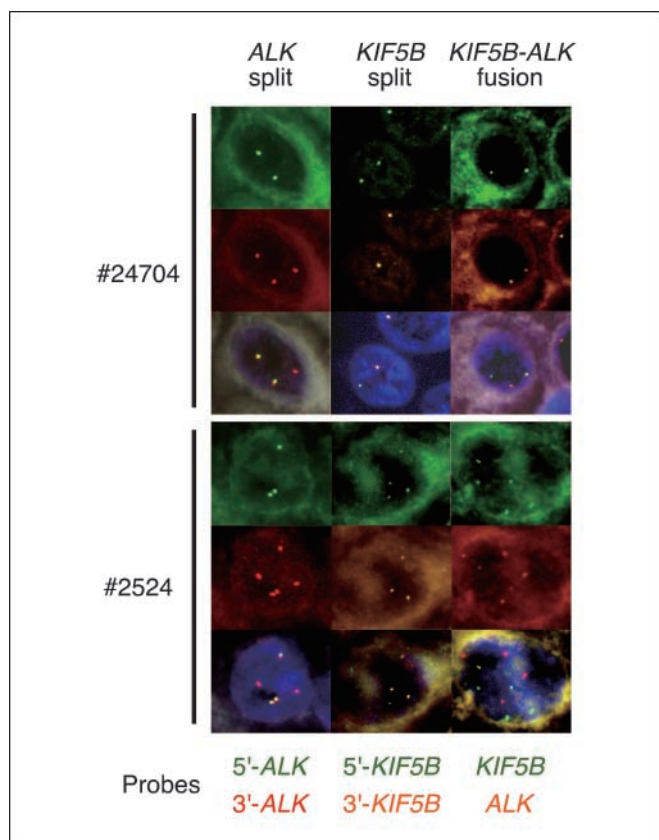
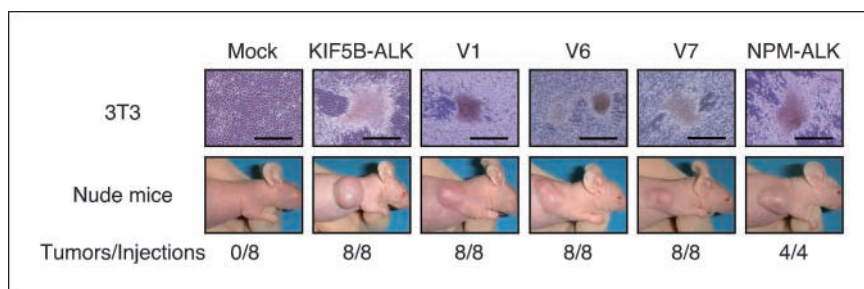


Fig. 4. Fluorescence *in situ* hybridization analysis of *KIF5B-ALK*. Sections of tumors positive for *KIF5B-ALK* (IDs #24704 and #2524) were subjected to fluorescence *in situ* hybridization with an *ALK* split assay (left), a *KIF5B* split assay (middle), or a *KIF5B-ALK* fusion assay (right). Bottom, the color of fluorescence for the BAC clones in each hybridization. Nuclei are stained blue with 4',6-diamidino-2-phenylindole.

⁵ <http://cgap.nci.nih.gov/sage/anatomicviewer>

Fig. 5. Transforming activities of EML4-ALK and KIF5B-ALK. *A*, mouse 3T3 fibroblasts were infected with retroviruses encoding KIF5B-ALK, NPM-ALK, or variant 1, 6, or 7 of EML4-ALK or with the corresponding empty virus (*mock*). The cells were photographed after culture for 14 d. *Scale bars*, 500 μ m. *B*, nude mice were injected s.c. with 3T3 cells infected as in *A*, and tumor formation was examined after 20 d. *Bottom*, the number of tumors formed per eight injections.



A fusion protein containing most of KIF5B and the intracellular (kinase) domain of the platelet-derived growth factor receptor A has been detected in idiopathic hyper-eosinophilic syndrome (18). The genome of some patients with this condition exhibits a chromosome translocation, t(4;10)(q12;p11), which results in the production of a KIF5B-PDGFR α fusion mRNA in which exon 23 of KIF5B is ligated to exon 12 of PDGFR α . Given that the KIF5B portion of KIF5B-platelet-derived growth factor receptor A contains six of the seven coiled-coil domains within the stalk region, the fusion protein likely dimerizes constitutively and thereby possesses transforming potential. KIF5B-ALK is thus the second example of an oncogenic KIF5B fusion to a PTK.

The subcellular localization of ALK fusion proteins likely depends on the fusion partner. For instance, whereas NPM-ALK, which is associated with anaplastic large cell lymphoma, is present in both the nucleus and cytoplasm, nuclear localization has not been detected for other ALK fusion proteins including CLTC-ALK, TPM3-ALK, TFG-ALK, ATIC-ALK (19), and EML4-ALK (5). The pattern of immunohistochemical staining for KIF5B-ALK did not resemble that of any of these other ALK fusion proteins. The observed perinuclear halo of KIF5B-ALK staining may indicate accumulation of the fusion protein at the periphery of the cytoplasm (subcell membrane region), possibly reflecting transport of KIF5B-ALK along microtubules. Signaling downstream of KIF5B-ALK may thus differ substan-

tially from that of other ALK fusion proteins, as exemplified by the differential phosphorylation of STAT proteins associated with these fusion proteins (19).

In conclusion, we have developed a modified immunohistochemical staining procedure for the detection of ALK and ALK fusion proteins in lung cancer that may prove suitable for screening purposes in pathology laboratories. Our identification of a second ALK fusion gene, KIF5B-ALK, in NSCLC further supports the clinical relevance of ALK in the pathogenesis of this disease. Given the recent development of several ALK inhibitors and their potential therapeutic efficacy for tumors positive for ALK fusion proteins (6, 10, 20), accurate diagnosis of tumors expressing activated ALK or ALK fusion proteins (5, 21, 22) will be essential to identify subgroups of patients who are suitable for treatment with such drugs.

Disclosure of Potential Conflicts of Interest

K.T. serves as a consultant to Dako.

Acknowledgments

We thank Motoyoshi Iwakoshi, Keiko Shiozawa, Tomoyo Kakita and Reimi Asaka for their technical assistance. The nucleotide sequences of the cDNAs for EML4-ALK variants 6 and 7 and for KIF5B-ALK have been deposited in the DDBJ/European Molecular Biology Laboratory/Genbank databases under the accession numbers AB462411, AB462412, and AB462413, respectively.

References

- Mitelman F. Recurrent chromosome aberrations in cancer. *Mutat Res* 2000;462:247–53.
- Bartram CR, de Klein A, Hagemeijer A, et al. Translocation of c-abl oncogene correlates with the presence of a Philadelphia chromosome in chronic myelocytic leukaemia. *Nature* 1983;306:277–80.
- Mitelman F, Johansson B, Mertens F. The impact of translocations and gene fusions on cancer causation. *Nat Rev Cancer* 2007;7:233–45.
- Kumar-Sinha C, Tomlins SA, Chinnaiyan AM. Recurrent gene fusions in prostate cancer. *Nat Rev Cancer* 2008;8:497–511.
- Soda M, Choi YL, Enomoto M, et al. Identification of the transforming EML4-ALK fusion gene in non-small-cell lung cancer. *Nature* 2007;448:561–6.
- Choi YL, Takeuchi K, Soda M, et al. Identification of novel isoforms of the EML4-ALK transforming gene in non-small cell lung cancer. *Cancer Res* 2008;68:4971–6.
- Inamura K, Takeuchi K, Togashi Y, et al. EML4-ALK fusion is linked to histological characteristics in a subset of lung cancers. *J Thorac Oncol* 2008;3:13–7.
- Takeuchi K, Choi YL, Soda M, et al. Multiplex reverse transcription-PCR screening for EML4-ALK fusion transcripts. *Clin Cancer Res* 2008;14:6618–24.
- Soda M, Takada S, Takeuchi K, et al. A mouse model for EML4-ALK-positive lung cancer. *Proc Natl Acad Sci U S A* 2008;105:19893–7.
- McDermott U, Sharma SV, Dowell L, et al. Identification of genotype-correlated sensitivity to selective kinase inhibitors by using high-throughput tumor cell line profiling. *Proc Natl Acad Sci U S A* 2007;104:19936–41.
- Rikova K, Guo A, Zeng Q, et al. Global survey of phosphotyrosine signaling identifies oncogenic kinases in lung cancer. *Cell* 2007;131:1190–203.
- Koivunen JP, Mermel C, Zejnullahu K, et al. EML4-ALK fusion gene and efficacy of an ALK kinase inhibitor in lung cancer. *Clin Cancer Res* 2008;14:4275–83.
- Cataldo KA, Jalal SM, Law ME, et al. Detection of t(2;5) in anaplastic large cell lymphoma: comparison of immunohistochemical studies, FISH, and RT-PCR in paraffin-embedded tissue. *Am J Surg Pathol* 1999;23:1386–92.
- Martelli MP, Sozzi G, Hernandez L, et al. EML4-ALK rearrangement in non-small-cell lung cancer and non-tumor lung tissues. *Am J Pathol* 2009;174:661–70.
- Sablin EP. Kinesins and microtubules: their structures and motor mechanisms. *Curr Opin Cell Biol* 2000;12:35–41.
- McLachlan CS, Jusuf PR, Rummery N, et al. Tyramide signal amplification enhances the detectable distribution of connexin-43 positive gap junctions across the ventricular wall of the rabbit heart. *Arch Histol Cytol* 2003;66:359–65.
- Pulford K, Morris SW, Turturo F. Anaplastic lymphoma kinase proteins in growth control and cancer. *J Cell Physiol* 2004;199:330–58.
- Score J, Curtis C, Waghorn K, et al. Identification of a novel imatinib responsive KIF5B-PDGFR α fusion gene following screening for PDGFR α overexpression in patients with hypereosinophilia. *Leukemia* 2006;20:827–32.
- Armstrong F, Duplantier MM, Tremat P, et al. Differential effects of X-ALK fusion proteins on proliferation, transformation, and invasion properties of NIH3T3 cells. *Oncogene* 2004;23:6071–82.
- McDermott U, Iafrate AJ, Gray NS, et al. Genomic alterations of anaplastic lymphoma kinase may sensitize tumors to anaplastic lymphoma kinase inhibitors. *Cancer Res* 2008;68:3389–95.
- Morris SW, Kirstein MN, Valentine MB, et al. Fusion of a kinase gene, ALK, to a nucleolar protein gene, NPM, in non-Hodgkin's lymphoma. *Science* 1994;263:1281–4.
- Chen Y, Takita J, Choi YL, et al. Oncogenic mutations of ALK kinase in neuroblastoma. *Nature* 2008;455:971–4.